Energy, Mines and Resources Canada | Énergie, Mines et Ressources Canada

CANMET

Canada Centre for Mineral and Energy Technology | Centre canadien de la technologie des minéraux et de l'énergie

HYSTERESIS CAUSED BY DIMENSIONAL CHANGES OF POROUS SOLIDS DURING MERCURY POROSIMETRY

M. Ternan and L.P. Mysak
HYDROCARBON PROCESSING RESEARCH LABORATORY

SEPTEMBER 1986

ENERGY RESEARCH PROGRAM
ENERGY RESEARCH LABORATORIES
DIVISION REPORT ERL/ERP 86-52(J)

HYSTERESIS CAUSED BY DIMENSIONAL CHANGES OF POROUS SOLIDS DURING MERCURY POROSIMETRY

by

Marten Ternan and Luigi P. Mysak

Energy Research Laboratories
Department of Energy Mines and Resources
Ottawa, Ontario, K1A0G1, Canada

SUMMARY

Hysteresis in mercury porosimetry is often attributed to differences in contact angle and to ink bottle shaped pores. In this paper the contribution to hysteresis from dimensional changes in pores is considered. Empty pores are compressed by the applied external mercury pressure. The mercury penetration pressure is related to the dimensions of the compressed pores. After the pores are filled with mercury, the pressure becomes isotropic throughout the solid and the pores revert to their original dimensions. The pressure at which

mercury retracts from the pores is related to the original pore dimensions. Using these concepts, the magnitude of the pore dimension changes was determined as a function of the applied mercury pressure, the modulus of elasticity of the solid and the solid porosity. The width of the hysteresis loop ($P_{pen} - P_{ret}$) was found to be minimal at pressures less than 10,000 psi (70 MPa). At 50,000 psi (350 MPa) the width of the hysteresis loop caused by dimensional changes can be significant even when the modulus of elasticity is large. The predicted hysteresis loop widths are compared with experimental data reported for model pore systems.

INTRODUCTION

The diameters of pores in catalysts and other porous solids are often measured using the mercury porosimetry technique. In this technique the solid is surrounded by mercury, the mercury pressure is increased, and the volume of mercury which penetrates the solid at each pressure is measured. Subsequently, the pressure is lowered and the volume of mercury which retracts from the solid is measured at each pressure. The mercury pressure, P_{Hg}, is related to the pore diameter, d_p, by the equation of Young and LaPlace (1), Equation 1,

$$d_p = \frac{4\ \bar{\sigma}_{LV} \cos \bar{\theta}}{P_{Hg}} \qquad (1)$$

where $\bar{\sigma}_{LV}$ is the surface tension of mercury at its liquid-vapour interface and $\bar{\theta}$ is the contact angle between the mercury liquid and the pore wall. The contact angle is usually assigned a value between

130 and 140 degrees. For example Balker and Relthaar (2) have measured mercury contact angles on 20 different catalysts, and found them all within this range. However, other values have been used occasionally (3).

Figure 1 shows a mercury porosimetry curve for a catalyst pellet of compressed solid particles. The hydrodesulphurization catalyst is composed of cobalt and molybdenum oxides supported on alumina, which is the major component. It is readily apparent that the pressure at which mercury penetrates the pores is greater than the pressure at which it retracts from the pores.

There are several well known contributions to this hysteresis phenomenon. One is that the contact angle is greater during penetration than during retraction. Experimental studies with liquids on flat surfaces (4) have shown that the advancing macroscopic contact angle is greater than the receding macroscopic contact angle. However, in some cases the microscopic contact angle is known to be different (5) than the macroscopic contact angle. Phenomena occurring inside a pore will likely include both these effects.

A second well known explanation for hysteresis during mercury porosimetry is that the pores have an ink bottle shape, that is a smaller diameter neck which is connected to a larger diameter body. According to the equation of Young and LaPlace a greater pressure would be required for mercury to penetrate the smaller neck. When the pressure is high enough to penetrate the small neck, mercury would fill both the neck and the body. During pore emptying, mercury would retract from the small diameter pore neck at a higher pressure and from the large diameter pore body at a lower pressure. According to this explanation the pore body would fill at high pressure and empty at low pressure, thereby explaining hysteresis. The gamma alumina catalyst support, used for the measurements in Figure 1, is considered to be composed of spherical particles approximately 3-50 nm in diameter (6,7). Spherical particles would be expected to pack in a

manner which would form both smaller pore necks and larger pore spaces.

Recently a third explanation for hysteresis has been suggested (8). The Van der Waals forces from the solid walls of the pores will interact with mercury atoms after the pore is filled. This interaction is not possible when the pores are empty. The summation of these forces, the pore potential, would cause the retraction pressure to be lower than the penetration pressure. In the opinion of some workers (9) the pore potential only makes a small contribution to hysteresis.

Thermal hysteresis is a fourth explanation. It has been shown experimentally (3) that the temperature of the solid sample and its surrounding mercury increases during penetration and decreases during retraction. Equipment to eliminate most of this effect has been described (3).

CALCULATIONS

In the present work, the contribution to hysteresis by the compression of the solid, is examined. The compressibility phenomenon is illustrated in Figure 2. The pressure within the solid will be P_{s1} where the solid contacts mercury in the bulk phase, P_{s2} where the solid contacts mercury inside a pore, and P_{s3} where the solid is in contact with vacuum inside a pore. During penetration, the mercury fluid surrounding the porous particle will be at pressure P_{Hg}. If the solid is isotropic, this pressure will be transmitted throughout the solid. The mercury fluid in the pores, which were filled previously during penetration, will also be at pressure P_{Hg}. However, the pore spaces which are still empty will be under vacuum. The pressure drop across the solid-vacuum interfaces of the

empty pore spaces, $\triangle P$, will be P_{Hg}. This pressure drop will cause a deformation, $\triangle$, of the pore radius, r_p. In contrast this pressure drop will not exist at the solid-fluid interfaces of the filled pore spaces.

During mercury retraction, the pore spaces will already have been filled with mercury. Therefore there will be no $\triangle P$ and no deformation, $\triangle$. During retraction the mercury will empty from pores of radius r_p at pressure P_{Hg}. However, during penetration, the pore radius will be smaller, $r_p - \triangle$, and therefore fill at a higher pressure than P_{Hg}. The change in dimension, $\triangle$, would cause the pores to fill at a higher pressure and empty at a lower pressure. Figure 2 shows the filled portion of the pore having radius r_p, and the empty portion of the pore under vacuum having radius $r_p - \triangle$.

There are at least two ways $\triangle$ can influence hysteresis. As already indicated by the equation of Young and LaPlace, any change in pore dimension will influence the pressure at which mercury penetrates into or retracts from pores. Secondly if the deformation of the solid is sufficiently great (at large mercury pressures), the solid can fracture. This will alter the structure of the pore space and thereby contribute to hysteresis.

A simplified model of a porous solid can be constructed as illustrated in Figure 3. It is a solid composed of straight parallel circular pores of radius r_p. The circles are spaced at the vertices of equilateral triangles having sides of length $2r_p + d$ where d is the distance between pores. For an element having the cross-sectional area described by the parallelpiped shown in Figure 3,

$$V_p = \epsilon V_T \qquad (2)$$

where V_p and V_T represent the volume of the pores and the total volume of the solid respectively. The porosity, ϵ, is the volume fraction of the solid occupied by pores. Equation 2 can be written in terms of the pore length, L, as

$$\pi r_p^2 L = \epsilon (2r_p + d)^2 \sin\theta L \qquad (3)$$

Setting $\theta = 60^\circ$ (for an equilateral triangle) and rearranging

$$\frac{d}{r_p} = \frac{1.905}{\sqrt{\epsilon}} - 2 \qquad (4)$$

The d/r_p ratio of a solid having this simplified pore structure was calculated from Equation 4 and is shown in Figure 4, as a function of porosity. It is seen that as the porosity of the solid, ϵ, approaches zero, the distance between the pores, d, becomes very large in comparison with the pore radius. Equation 4 can be used to calculate the d/r_p ratio of a simplified solid which has a porosity corresponding to that of any real porous solid.

In order to calculate the value of $\triangle$ for the simplified pore structure, an analogy can be made. The vacuum within the pore of a solid subjected to mercury pressure, can be compared to a thick walled cylindrical pressure vessel, having an external pressure and an internal vacuum. The equation describing the deformation, $\triangle$, of the

vessel's interior wall is well known (10)

$$\frac{\Delta}{r_i} = \frac{2 P r_e^2}{E(r_e^2 - r_i^2)} \qquad (5)$$

where P is the external pressure, and E is the modulus of elasticity. By analogy the vessel internal radius, r_i in Equation 5, can be identified with the pore radius, r_p, and the external vessel radius, r_e, arbitrarily set equal to $r_p + d$, to produce Equation 6,

$$\frac{\Delta}{r_p} = \frac{1}{C} \frac{P_{Hg}}{E} \qquad (6)$$

where

$$C = \frac{1}{2} \left[1 - \frac{1}{(1 + d/r_p)^2} \right] \qquad (7)$$

The term Δ/r_p is the strain, and P_{Hg} is the stress. For a

non-porous material the proportionality constant between these two is the modulus of elasticity, E. For porous materials, the proportionality constant is modified somewhat, as shown in Equation 7. By substituting the d/r_p ratio from Equation 4 into Equation 7, the proportionality constant, C, can be expressed in terms of the solid porosity, ϵ, as shown in Figure 5.

RESULTS AND DISCUSSION

The strain calculated using Equation 6, is shown in Figure 6 for two different values of E. It is seen that for any given stress, P_{Hg}, the strain increases with increasing porosity of the solid. Also the strain is larger for more elastic materials (those with smaller E values).

For any solid porosity, ϵ, Equation 6 can be used in conjunction with Equation 1 to calculate the width of the hysteresis loop. For a specified pore radius, r_p, the mercury retraction pressure, P_{ret}, can be calculated from Equation 1. This corresponds to an undeformed pore when the pressure in the solid is equal to the pressure of the mercury fluid within the pore, as illustrated in Figure 2. Next the deformation, $\triangle$, prior to mercury penetration can be calclulated from Equation 6. The pore radius just prior to mercury penetration, $r_p - \triangle$, can then be used to calculate the mercury penetration pressure, P_{pen}, again using Equation 1. The width of the hysteresis loop is shown in Figure 7 as a function of porosity ϵ, for solids having two different moduli of elasticity.

The alumina catalyst support, shown in Figure 1, would be expected to have a modulus of elasticity of approximately 10^7 psi and a porosity of 0.5. Applying these parameters to the upper portion of Figure 7, it is apparent that the portion of the hysteresis loop caused by dimensional changes of the pores would be less than 1 k psi.

Since Figure 1 indicates that the total width of the hysteresis loop is approximately 20 k psi, it appears that dimensional changes in this pore structure have a small but significant influence on the width of the hysteresis loop.

The real structure of gamma alumina catalyst supports is usually considered to be an assembly of spheres, not the simplified pore structure of Figure 3. An assembly of spheres is equivalent to a collection of ink bottle shaped pores. Therefore, pore shape would be expected to make a large contribution to hysteresis. This is consistent with the hysteresis caused by dimensional changes being small compared to hysteresis caused by other factors, such as varying pore shape (11), or perhaps contact angle (12).

The influence of pore shape is not present in Nucleopore filters (13,14). They are fabricated from polycarbonate, and have straight circular pores, which are very close to the model shown in Figure 3. They have low porosity and the modulus of elasticity for polycarbonate is 3×10^5 psi. The lower portion of Figures 6 and 7 show the deformation (strain) and the hysteresis observed with these materials (13,14). The width of the hysteresis loop caused by dimensional change has been taken from Figure 7 and compared with literature data (13,14) in Figure 8. The solid line in Figure 8 represents no hysteresis, that is the mercury penetration pressure is identical to the mercury retraction pressure. The dotted lines indicate that a small but significant amount of hysteresis is predicted from dimensional changes. The experimental data points indicate that there is a large amount of hysteresis that can not be accounted for by dimensional changes of the pores. The ink bottle explanation of hysteresis is not applicable since straight pores do not form an ink bottle shape. The experimental data in Figure 6 have been explained (12) in terms of different contact angles for penetration and retraction. The conclusion for both materials, hydrodesulphurization catalyst and polycarbonate filters is the same, that dimensional changes of the pores have a small but significant

influence on the hysteresis phenomenon.

The width of the hysteresis loop can be altered substantially if fracture of the porous solid occurs. Literature data for alumina (15-19) indicate that fracture occurs when the strain exceeds 0.013. For the hydrodesulphurizaton catalyst ($\epsilon = 0.5$) the strain, from Figure 6, just reaches this value when the external pressure is slightly below 50 k psi. Therefore fracture probably does not occur to any appreciable extent with this porous solid. This conclusion is consistent with experimental results for alumina reported elsewhere (20).

Fracture does occur in some porous solids. The results in Figure 6 suggest that fracture is more important for higher porosity solids. One example(21) occurred with a magnesium trisilicate ($2MgO.3SiO_2.H_2O$) catalyst support. Part of the retraction occurred at higher pressures than the corresponding mercury penetration. This phenomenon is probably caused by the fractured pores having smaller dimensions than the original ones.

In summary, changes in pore dimensions caused by large external pressures of mercury make a small but appreciable contribution which has been ignored in virtually all mercury porosimetry literature published to date. The contribution of dimensional changes to hysteresis in the solids considered here is overshadowed by other factors. However the results in Figures 6 and 7 indicate that, at high pressures, in solids having large porosities and low moduli of elasticity, dimensional changes will make large contributions to hysteresis. Secondly, it seems likely that some materials (certain combinations of porosity and moduli of elasticity) will fracture when subjected to high pressure. Fracture phenomena will change the pore dimensions and also contribute to hysteresis.

REFERENCES

1. P.R. Pujado, C. Huh, and L.E Scriven, J. Colloid Interf. Sci. 38 ,(1972)662-663.
2. A. Balker, and A. Relthaar, Ind. Eng. Chem. Prod. Res. Dev. 21 ,(1982)590-591.
3. R.W. Smithwick and E.L. Fuller, Powder Technol., 38 (1984)165-173.
4. R.H. Dettre, and R.E. Johnson, (a) Adv. Chem. No. 43, Am. Chem. Soc., Washington, D.C., (1964); (b) J. Phys. Chem. 69 (1965)1507.
5. R.L. Patrick and J.A. Brown, J. Colloid Interf. Sci. 35 (1971)362-363.
6. J. Turkevitch and J. Hillier, Anal. Chem. 21 (1985)475.
7. M.F.L. Johnson and J. Mooi, J. Catal. 10 (1968)342.
8. S. Lowell, Powder Technol., 25 (1980)37-43.
9. W.C. Conner A.M. Lane, and A. J. Hoffman, J. Colloid Interf. Sci. 100 (1984)185-193.
10.. J.F. Harvey, Pressure Vessel Design, Van Nostrand, Princeton, 1963, p. 51.
11. R.G. Jenkins and M.B. Rao, Powder Technol. 38 (1984)177.
12. S. Lowell and J.E. Shields, Powder Technol. 38 (1984)121.
13. A.A. Liabastre and C. Orr, J. Colloid Interf. Sci., 64 (1978)1.
14. M. Ternan and O. M. Fuller, Can. J. Chem. Eng. 57 ,(1979)750.
15. J.E.Bailey and N. A. Hill, Proc. Brit. Ceram. Soc. 15 ,(1970)15-35.
16. J.S. Florry and B. Robson, Proc. Brit. Ceram. Soc., 25 (1975)27-38.
17. M. Ternan, Can. J. Chem. Eng. 61 (1983)689-696.
18. F.P. Knudsen, J. Am. Ceram. Soc. 45 (1962)94-95.
19. Wang, J.C., J. Mater. Sci. 19 (1984)809-814.
20. D.N. Winslow, J. Colloid Inter. Sci., 67 (1978)42-47.

21. M. Ternan, R.H. Packwood, R. M. Buchanan, and
B.I. Parsons, Can. J. Chem. Eng., 60 (1982)33-39.

LEGENDS FOR ILLUSTRATIONS

Figure 1 Mercury porosimetry curves for the oxide form of a cobalt-molybdenum-gamma alumina catalyst. Volume of mercury (mL/g) versus applied external pressure (k psi). Squares are for penetration. Triangles are for retraction.

Figure 2 Dimensional changes in pore radius caused by subjecting the solid to high pressure while the pore interior is under vacuum.

Figure 3 Pore system model of straight round cylindrical pores which are uniformly spaced.

Figure 4 d/r_p (distance between pores/pore radius) versus porosity (volume fraction of the solid occupied by pores).

Figure 5 Proportionality constant C versus porosity. The constant C relates the elongation per unit length to the external pressure divided by the modulus of elasticity.

Figure 6 Strain (Δ/r_p) versus external pressure (k psi) for solids of various porosities. Results are shown for two moduli of elasticity (10^7 and 3×10^5 psi) (1 psi = 6.895 kPa).

Figure 7 Width of hysteresis loop (penetration pressure minus retraction pressure) versus applied external mercury pressure (k psi) (1 psi = 6.895 kPa).

Figure 8 Mercury retraction pressure versus mercury penetration pressure for various values of porosity C. Experimental data for polycarbonate filters are from ref. 8 (triangles) and ref. 9 (circles).

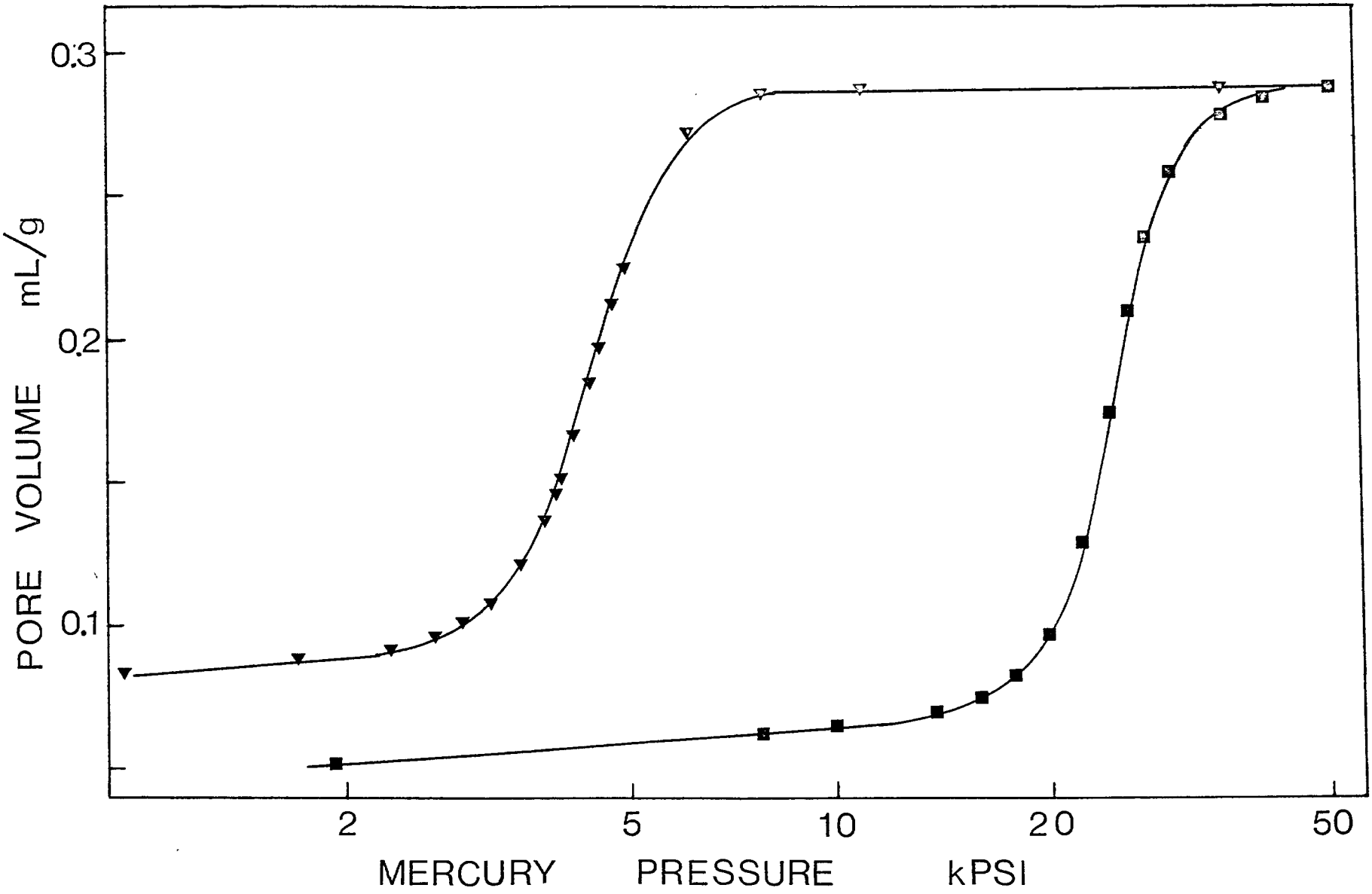
0.3
0.2
0.1
PORE VOLUME mL/g
2
5
10
20
50
MERCURY PRESSURE kPSI

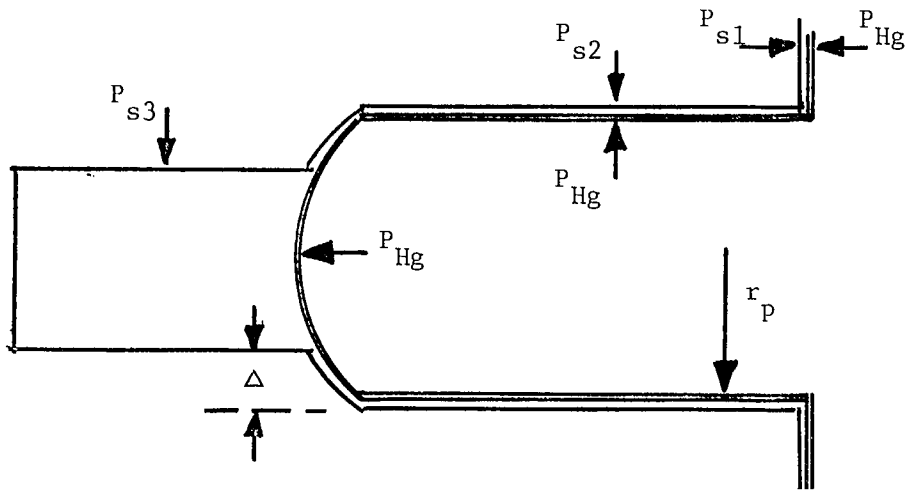
P_{s2}
P_{s1}
P_{Hg}
P_{s3}
P_{Hg}
P_{Hg}
r_p
Δ

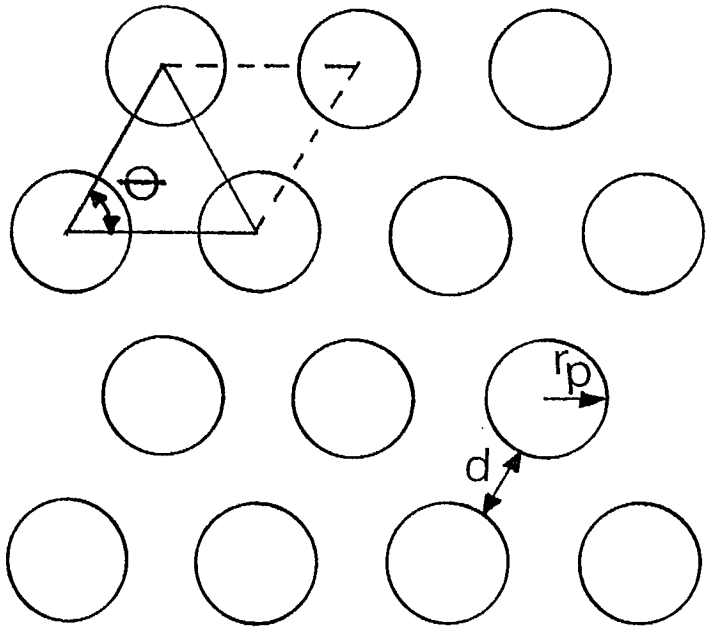
θ
rp
d

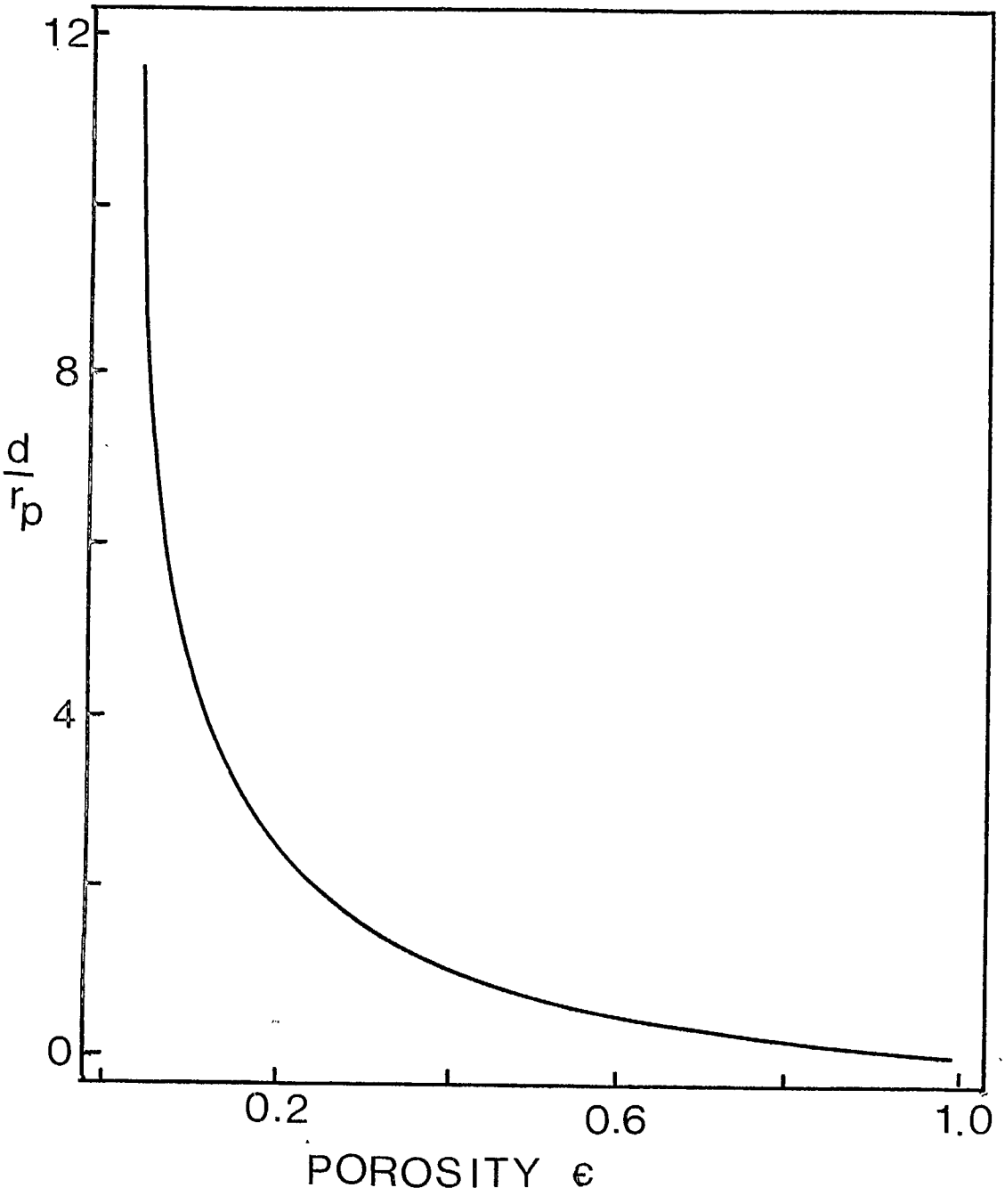

FIG 4

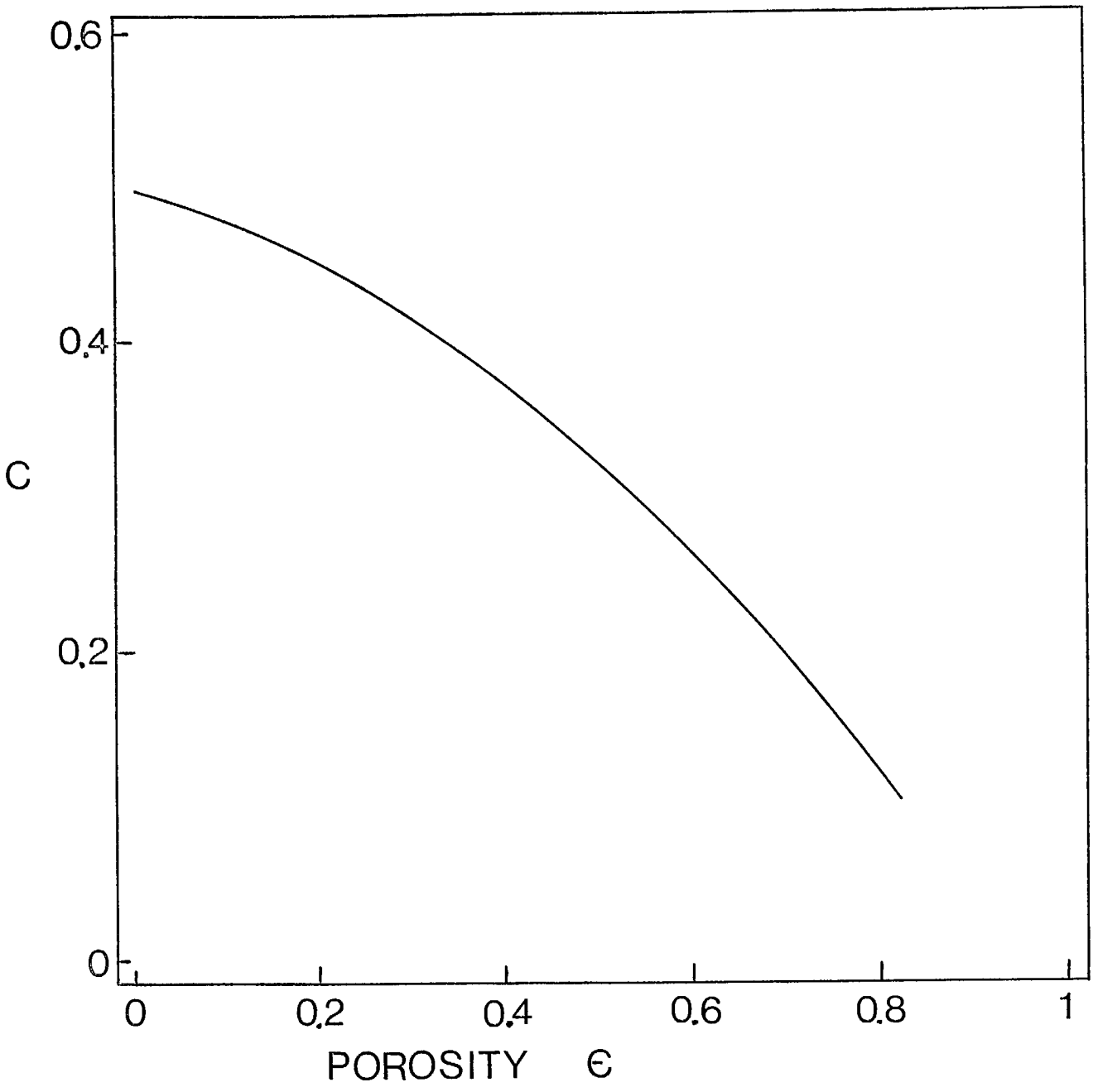

FIG 5

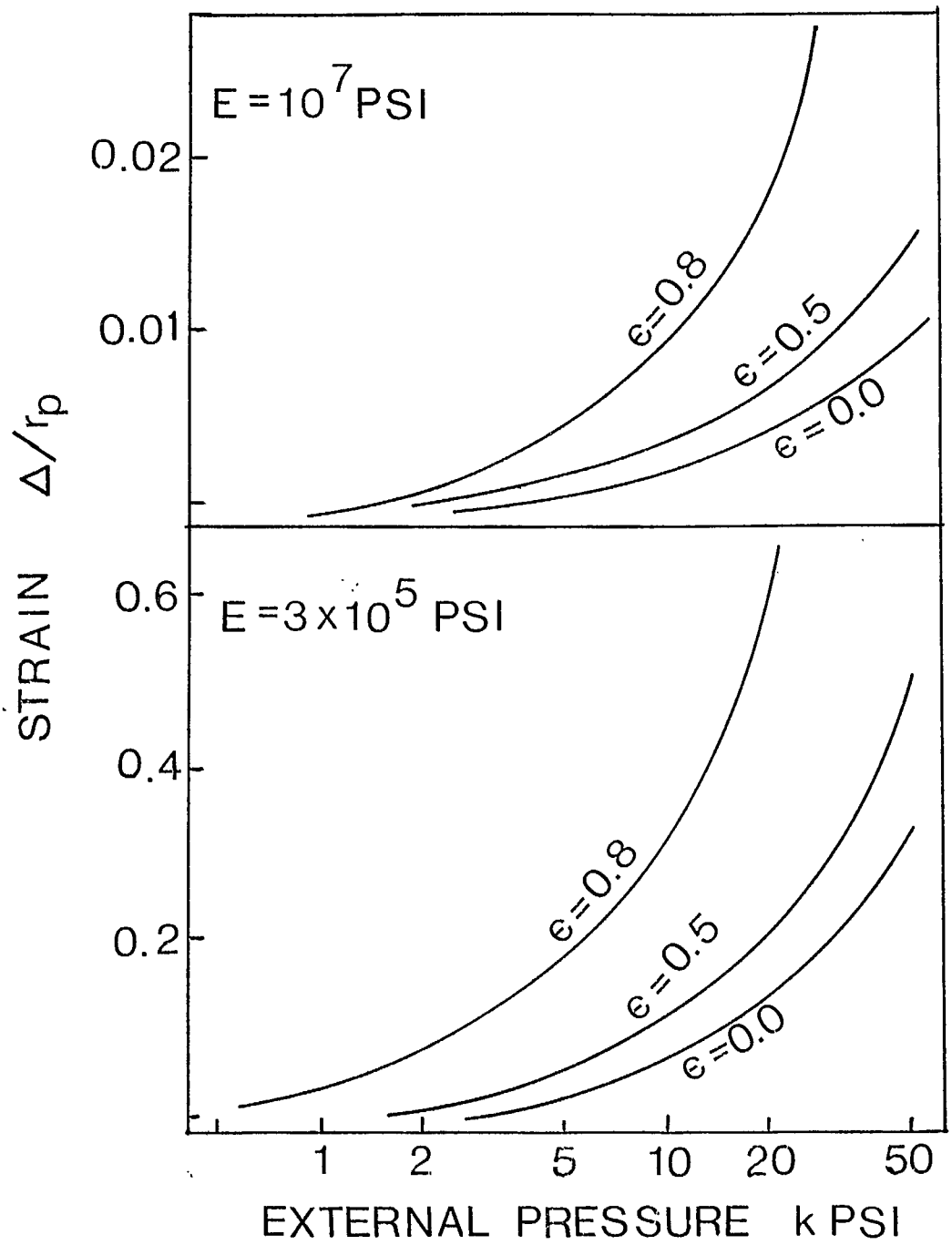
E = 10^7 PSI
0.02
0.01
ε=0.8
ε=0.5
ε=0.0
E = 3 x 10^5 PSI
0.6
0.4
0.2
ε=0.8
ε=0.5
ε=0.0
STRAIN Δ/r_p
1
2
5
10
20
50
EXTERNAL PRESSURE k PSI

F:36

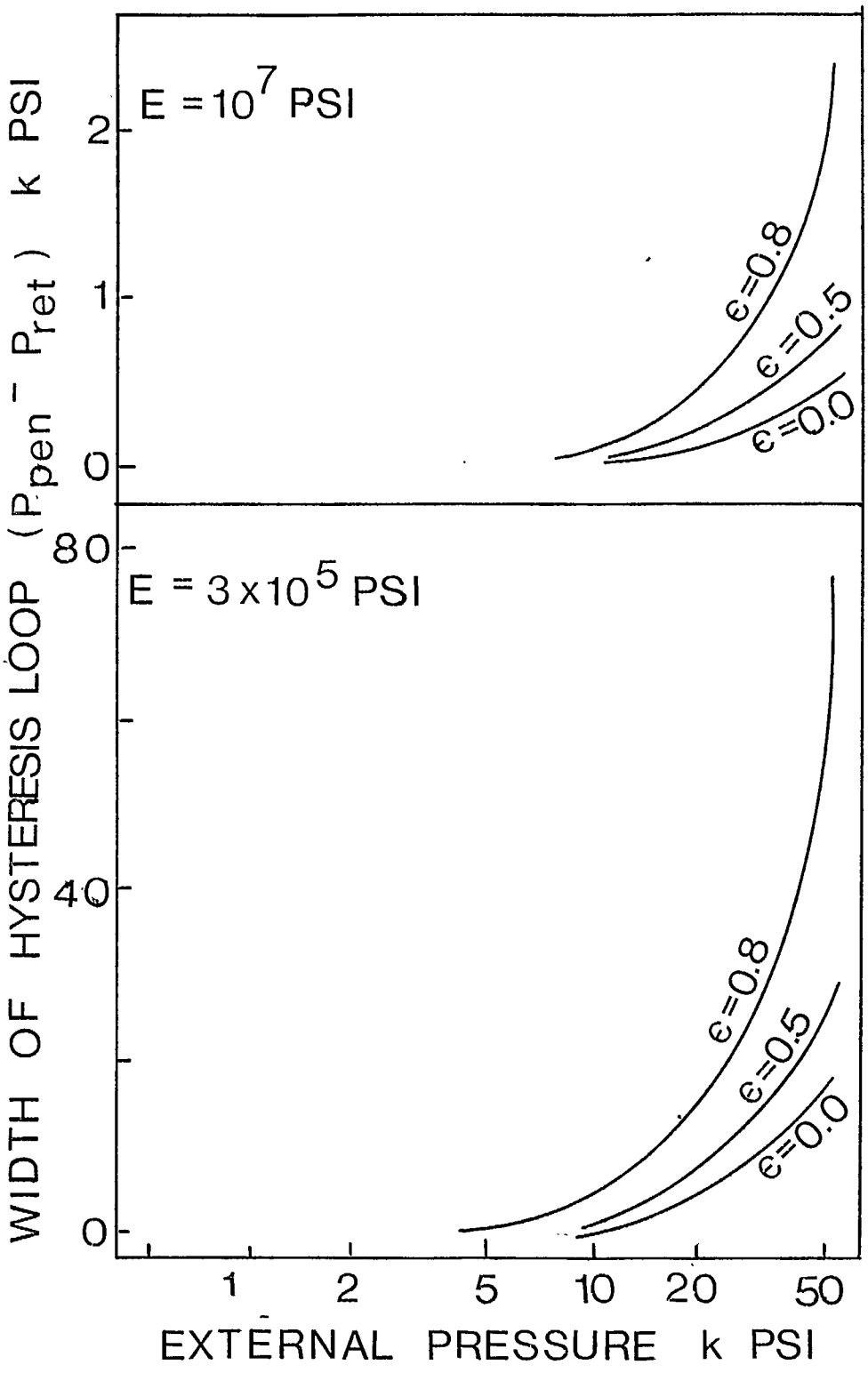
E = 10^7 PSI
E = 3 x 10^5 PSI
ε=0.8
ε=0.5
ε=0.0
WIDTH OF HYSTERESIS LOOP (P_pen - P_ret) k PSI
EXTERNAL PRESSURE k PSI
0
1
2
40
80
1
2
5
10
20
50

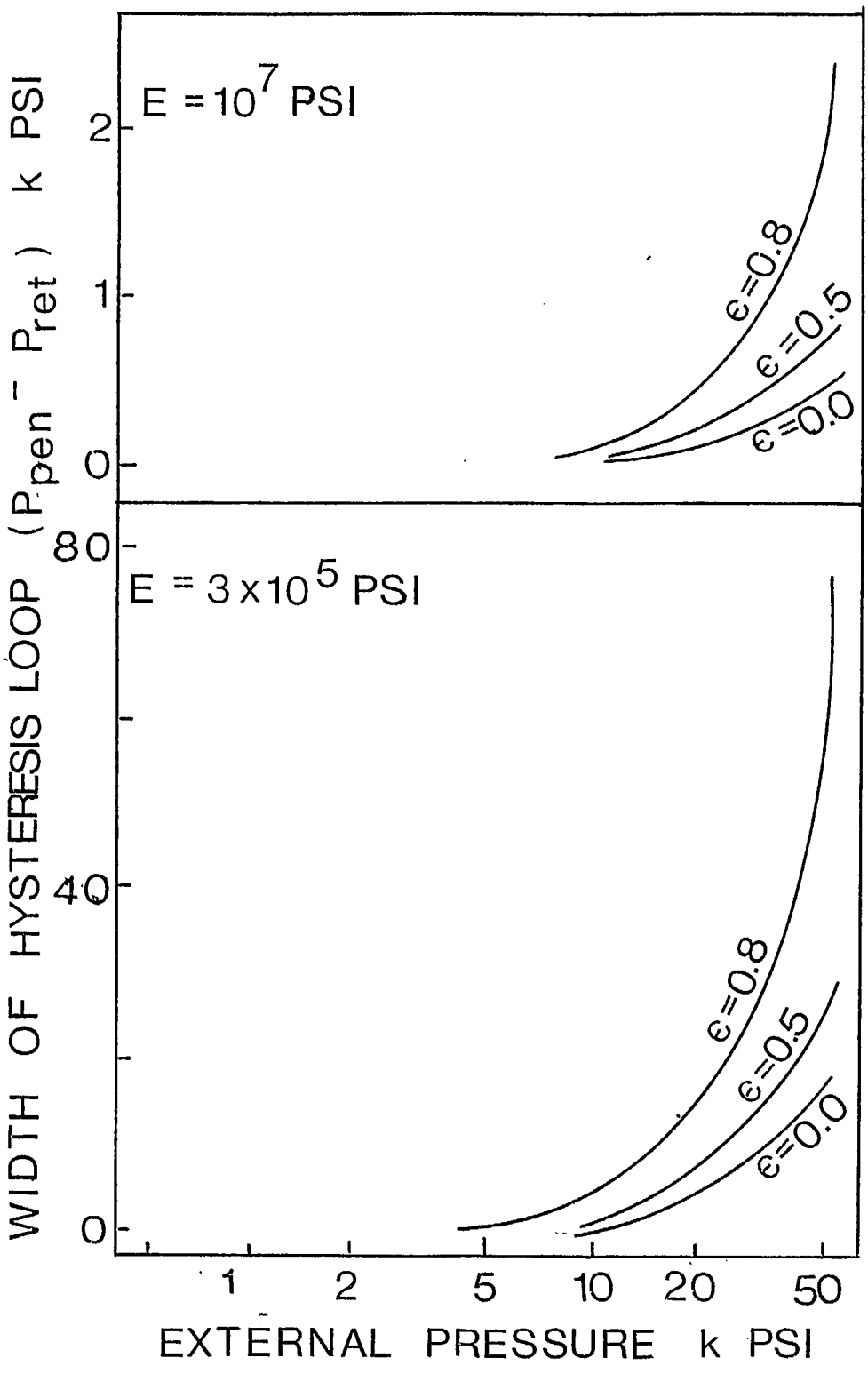
E = 10^7 PSI
E = 3 x 10^5 PSI
ε=0.8
ε=0.5
ε=0.0
WIDTH OF HYSTERESIS LOOP (P_pen - P_ret) k PSI
EXTERNAL PRESSURE k PSI
0
1
2
40
80
1
2
5
10
20
50

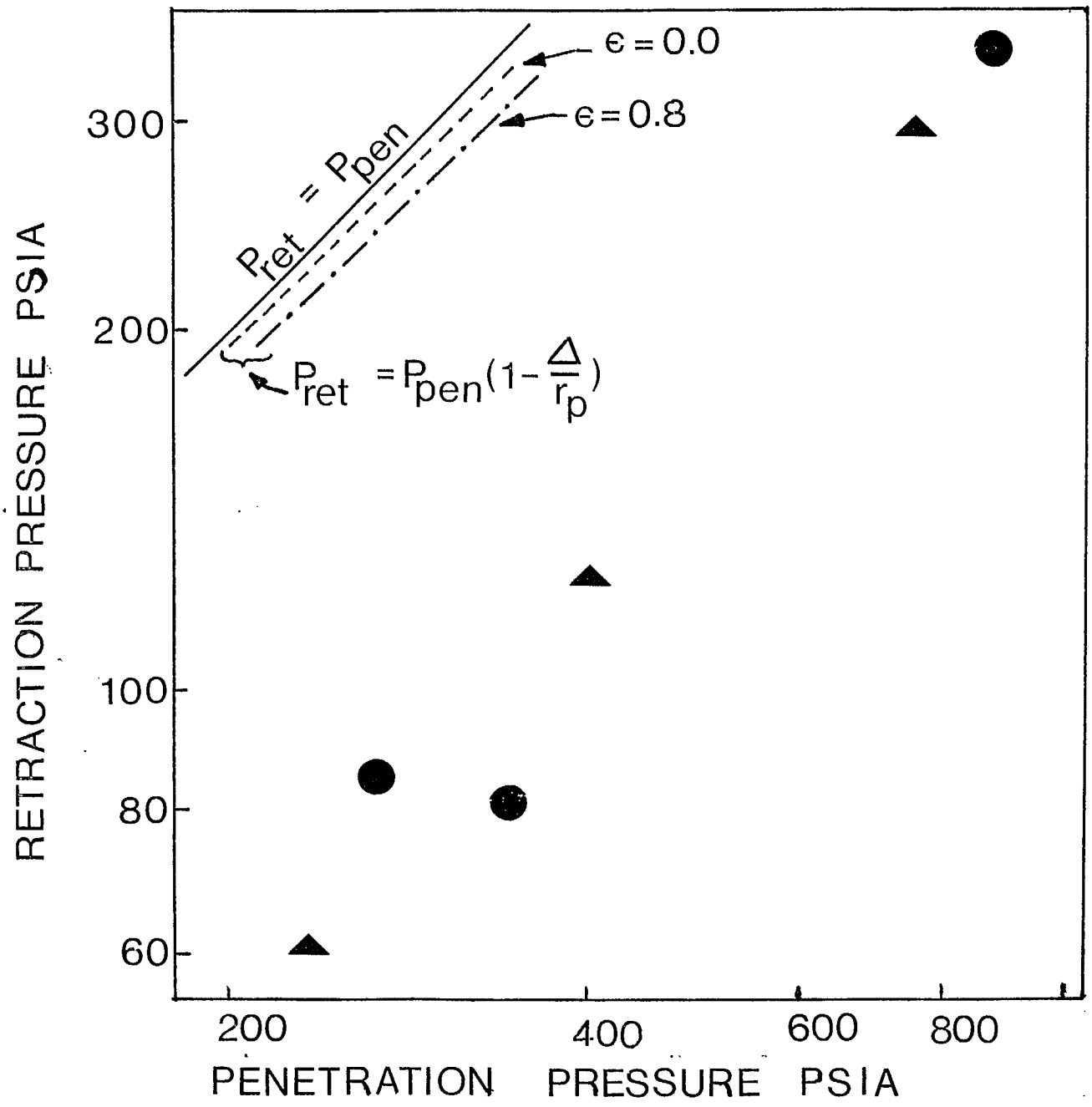
ε = 0.0
ε = 0.8
$P_{ret} = P_{pen}$
$P_{ret} = P_{pen}(1 - \frac{\Delta}{r_p})$
300
200
100
80
60
RETRACTION PRESSURE PSIA
200
400
600
800
PENETRATION PRESSURE PSIA

FIG 8